THE UNIVERSITY OF SYDNEY

Economics Working Paper Series

2014 - 05

International Wheat Price Responses to ENSO Shocks: Modelling Transmissions Using Smooth Transitions

David Ubilava

August 2014

International Wheat Price Responses to ENSO Shocks: Modelling Transmissions Using Smooth Transitions

David Ubilava*

School of Economics
University of Sydney

This Draft:† August 20, 2014

Abstract

Climate anomalies affect agricultural production in different parts of the world and can impact price behavior of internationally traded commodities. This research examines the effect of a particular climate phenomenon, El Niño Southern Oscillation (ENSO), on wheat prices from the major exporting regions. The study adopts a smooth transition modelling framework to addresses nonlinear dynamics and asymmetric price transmissions in response to the climate anomalies. Results suggest that a positive ENSO shock, i.e. El Niño, reduces wheat prices, while a negative ENSO shock, i.e. La Niña, increases wheat prices. The price changes vary across the export regions, but on average are within the three percent magnitude. The price increase due to La Niña is of a larger magnitude as compared to the price decrease due to El Niño. Moreover, price responses to ENSO shocks are more amplified (up to seven percent) during the La Niña regime, as compared to the El Niño regime. These findings are indicative of and consistent with the economics of grain price volatility and the theory of storage.

Keywords: Asymmetric Dynamics; El Niño Southern Oscillation; International Wheat Prices; Smooth Transition Modelling.

JEL Codes: C51; E31; Q11; Q54.

*E-Mail: david.ubilava@sydney.edu.au

†I thank seminar audience at the USDA/ERS Market and Trade Economics Division, as well as conference participants at the IAMO Forum 2014 in Haale, Germany, and at the AAEA 2014 Annual Meeting in Minneapolis, MN, USA, for their helpful comments and suggestions.

1 Introduction

The 2012 United States drought of historic magnitudes, followed by the record-setting temperatures in Australia, heated up the discussion about the climate change and its economic consequences. The increased incidence of extreme weather events is likely to be a byproduct of the global weirding (Rosenzweig et al., 2001; Friedman, 2010). For example, a prolonged La Niña phase of the ENSO cycle during the 2011–2012 period, has been cited as the potential common source of the aforementioned weather extremes in both hemispheres (e.g., Mallya et al., 2013). If ENSO truly plays the role of a "weather synchronizer" in different parts of the world, its economic effects may indeed be aggravating. The aforementioned is particularly relevant for the market dynamics of the internationally traded agricultural commodities. This study is concerned with assessing the influence of ENSO shocks on world wheat price behavior.

Wheat is one of the most important internationally traded cereals in the world. Notably, the world wheat market is characterized by a small number of large exporters. Approximately two–thirds of the internationally traded wheat is supplied by the United States, European Union, Australia, Canada, and Argentina. Such a high concentration in production, first of all, implies the potential of exercising a market power by the exporters. Indeed, previous studies have addressed the topics of the oligopolistic behavior of wheat exporters, the spatial arbitrage opportunities, and the law of one price hypotheses (e.g., Goodwin and Schroeder, 1991; Mohanty et al., 1995, 1999; Bessler et al., 2003). The high concentration also suggests that the wheat–exporting regions may be susceptible to ENSO-induced common weather shocks. While several studies have addressed the production effect of ENSO shocks (e.g., Nicholls, 1985; Legler et al., 1999; Selvaraju, 2003), little has been done to quantitatively examine the impact of the climate anomaly on international wheat price dynamics. The current research aims to fill this gap in the literature.

There has been growing interest in the role of the climate change on climate anomalies (e.g., Timmermann et al., 1999), and, in turn, the effect of climate anomalies on economic performance (e.g., Brunner, 2002). Climate anomalies are the medium-frequency quasi-cyclical deviations from the average climatic conditions. In the case of ENSO, the two extreme anomalies are *El Niño*, which denotes a positive deviation and is associated with warming sea-surface temperatures in the

equatorial Pacific, and *La Niña*–the counterpart of El Niño. When the ENSO cycle is at its long-run mean, the condition is known as *normal* or *neutral*. El Niño and La Niña can amplify weather conditions in different parts of the world, causing severe damages to production and infrastructure (e.g., Ropelewski and Halpert, 1987; Rosenzweig et al., 2001), with considerable socio-economic implications (Brunner, 2002; Hsiang et al., 2011).

Because ENSO events can negatively impact agricultural production, the causal connection between the climate anomaly and the commodity prices is merely an economic corollary. Indeed, several previous studies have examined the relationship between the ENSO events and the agricultural commodity price behavior. Among others, Keppenne (1995) reported statistically significant correlation between ENSO anomalies (especially La Niña) and soybean futures prices. Brunner (2002) found food and agricultural commodity prices to be highly responsive to ENSO variations. Laosuthi and Selover (2007) reported a statistically significant ENSO effect on price inflation of maize, sorghum, rice, palm oil, and coconut oil. Ubilava and Holt (2013) linked major vegetable oil price dynamics to the ENSO shocks.

Wheat is not an exception in regards to potential ENSO effects. Anecdotal evidence, supported by empirical findings, indicates a possibility of causal links between ENSO shocks and wheat price behavior. First of all, the relationship can be supply–driven, especially because much of the exported wheat is produced in just a few regions, where ENSO events can amplify unfavorable weather conditions. For example, droughts are common in the northern wheat belt of Australia during the El Niño conditions, while La Niña events can cause flooding rains in the region. Alternatively, La Niña events can induce droughts in the United States and Argentina. Overall, Iizumi et al. (2014) find that La Niña reduces global wheat yield by approximately four percent, while the effect of El Niño is half as pronounced. In addition to these "direct" supply shocks, ENSO-related weather hazards (e.g., flooding or frosts) may have "indirect" supply effect, resulting in damaged or malfunctioning infrastructure, and disturbing the timely transportation and delivery of grains from a seller to a buyer. Furthermore, the ENSO–wheat price relationship can also be demand-driven. For example, China and India are two of the largest producers and consumers of wheat, and normally are self-sufficient. ENSO-induced weather events, however, may damage crops (e.g.,

Selvaraju, 2003), thus turning these nations into the wheat importers during those years. This, of course, will put an upward pressure on the international wheat prices. Finally, because ENSO has become one of the better-known climate anomalies, economic agents, such as farmers, merchants, or even speculators, may adjust their positions on the futures market in response to ENSO-related news (e.g., Critchlow, 2014). Any resulted dynamics of the futures prices will have implications for spot prices as well.

The foregoing discussion suggests that the effect of the extreme ENSO events on world wheat prices may not be trivial. And, even though, quantifying the ENSO–wheat price dynamics is an interesting exercise of its own, this study makes an extra effort to assess the possibly nonlinear relationship between the ENSO anomalies and the vector of wheat prices. There are a number of reasons to believe that the price transmission in global wheat markets, as well as the effect of ENSO cycles on this relationship, can be nonlinear. First of all, ENSO cycles are characterized by asymmetric behavior (e.g., Hall et al., 2001; Ubilava and Helmers, 2013). In addition, the ENSO impact is not necessarily symmetric, i.e. weather conditions in a given region may be correlated with one of the ENSO phases, but not the other (Legler et al., 1999; Mason and Goddard, 2001, e.g.,). Furthermore, commodity price cycles reveal nonlinearities in terms of their magnitude and duration (Cashin et al., 2002). Finally, while the international prices of homogeneous commodities are closely linked due to trade and arbitrage activities (Goodwin and Schroeder, 1991), transaction costs may mitigate their co-movement within the so-called "neutral band" (Goodwin and Piggott, 2001). Because of the perceived nonlinearities, adequate modelling techniques should be applied to properly examine wheat price dynamics.

This research adopts a vector smooth transition autoregression (VSTAR) to address regime-dependent asymmetries in ENSO and wheat price dynamics (e.g., Rothman et al., 2001; Camacho, 2004). The VSTAR is a multivariate extension of the smooth transition autoregression (STAR), originally proposed as the smooth threshold autoregression by Chan and Tong (1986), with the subsequent modelling and testing frameworks developed and popularized in a series of papers by Luukkonen et al. (1988); Teräsvirta and Anderson (1992); Teräsvirta (1994); Eitrheim and Teräsvirta (1996). Finally, the STAR framework is a generalization of the threshold autoregression

of Tong and Lim (1980). The smooth transition modelling framework is readily applicable to address nonlinear commodity price dynamics, and has been successfully used in the literature (e.g., Holt and Craig, 2006; Balagtas and Holt, 2009; Goodwin et al., 2011). Additionally, this study adopts the generalized impulse response functions of Koop et al. (1996) to illustrate asymmetries in ENSO and wheat price cycles in response to the ENSO anomalies.

The rest of the paper is organized as follows. The study first briefly describes the modelling and testing frameworks of smooth transition models. It then introduces the data used in this research, followed by the results section, which presents estimated models, highlighting the advantages of nonlinear modelling from the statistical standpoint. The research then turns to the generalized impulse–response analysis to better illustrate economic significance of the ENSO effect on wheat price dynamics, including asymmetric price responses due to nonlinearities in ENSO cycles and the system of price equations. Finally, the concluding section highlights the main findings and the relevance of this study.

2 The Econometric Model and Linearity Tests

Let $\boldsymbol{x}_t = (x_{1,t}, x_{2,t}, \ldots, x_{n,t})'$ be a vector of endogenous variables, with a dynamic relationship given by a vector autoregression of order p, VAR(p):

$$\boldsymbol{x}_t = \boldsymbol{\alpha} + \sum_{i=1}^{p} B_i \boldsymbol{x}_{t-i} + \boldsymbol{\varepsilon}_t \tag{1}$$

where $\boldsymbol{\alpha}$ is a n-dimensional vector of parameters, and B_i, $i = 1, \ldots, p$, are n-dimensional matrices of parameters; finally, $\boldsymbol{\varepsilon}_t \sim iid\,(\mathbf{0}, \Sigma_\varepsilon)$, where Σ_ε is the residual covariance matrix.

Equation (1) can be extended to a nonlinear alternative in many different ways. For the purposes of current research, consider an additive nonlinear vector autoregression:

$$\boldsymbol{x}_t = \boldsymbol{\alpha}_0 + \sum_{i=1}^{p} B_{i,0} \boldsymbol{x}_{t-i} + \sum_{k=1}^{K} \left[\Gamma_k \left(\boldsymbol{\alpha}_k + \sum_{i=1}^{p} B_{i,k} \boldsymbol{x}_{t-i} \right) \right] + \boldsymbol{\varepsilon}_t, \tag{2}$$

where K denotes the maximum number of additive regimes, and Γ_k are n-dimensional diagonal

matrices of transition functions, each bounded between 0 and 1. Assume a two-regime model (i.e. set $K = 1$) and consider a transition function of the following form:

$$G\left(s_t;\gamma,\mathbf{c}\right) = \left\{1 + \exp\left[-\gamma_m/\sigma_{s_t}^m \prod_m \left(s_t - c_m\right)^m\right]\right\}^{-1} \tag{3}$$

where s_t is the regime-switching transition variable, and γ and $\boldsymbol{c}$ are parameters defining the shape of the transition function; σ_{s_t} is the standard deviation of the transition variable. Equation (2) coupled with equation (3) results in a multivariate variant of a family of smooth transition autoregressions. Further, by setting $m = 1$ one can obtain the so-called *logistic* transition function–the most popular application in the smooth transition modelling literature (e.g., Weise, 1999; Rothman et al., 2001; Camacho, 2004).

At this point assume $\boldsymbol{x}_t = (\boldsymbol{y}_t', z_t)'$, where $\boldsymbol{y}_t = (y_{1,t}, y_{2,t}, \ldots, y_{n-1,t})'$ is a vector of endogenous variables, and z_t is weakly exogenous to $\boldsymbol{y}_t$. For convenience, let's disentangle the exogenous equation from the system of endogenous equations, and rewrite equation (1) as follows:

$$\boldsymbol{y}_t = \tilde{\boldsymbol{\alpha}} + \sum_{i=1}^{p} \tilde{B}_i \boldsymbol{y}_{t-i} + \sum_{i=1}^{p} \tilde{\boldsymbol{\beta}}_i z_{t-i} + \boldsymbol{\varepsilon}_{y,t} \tag{4}$$

$$z_t = \alpha + \sum_{i=1}^{p} \beta_i z_{t-i} + \varepsilon_{z,t} \tag{5}$$

where $\tilde{\boldsymbol{\alpha}}$ and $\tilde{B}_i$ are $n-1$-dimensional vector and matrices, respectively, and $\tilde{\boldsymbol{\beta}}_i = (\beta^z_{y_1,i}, \ldots, \beta^z_{y_{n-1},i})'$ denotes the vector of causal parameters from $\{z_t\}$ to $\{\boldsymbol{y}_t\}$. A two-regime smooth transition version of these models is given by:

$$\begin{aligned}\boldsymbol{y}_t =& \tilde{\boldsymbol{\alpha}}_0 + \sum_{i=1}^{p} \tilde{B}_{i,0} \boldsymbol{y}_{t-i} + \sum_{i=1}^{p} \tilde{\boldsymbol{\beta}}_{i,0} z_{t-i} + \\ &+ \left(\tilde{\boldsymbol{\alpha}}_1 + \sum_{i=1}^{p} \tilde{B}_{i,1} \boldsymbol{y}_{t-i} + \sum_{i=1}^{p} \tilde{\boldsymbol{\beta}}_{i,1} z_{t-i}\right) G\left(s_{y,t};\gamma_y,c_y\right) + \boldsymbol{\varepsilon}_{y,t}\end{aligned} \tag{6}$$

$$z_t = \alpha_0 + \sum_{i=1}^{p} \beta_{i,0} z_{t-i} + \left(\alpha_1 + \sum_{i=1}^{p} \beta_{i,1} z_{t-i}\right) G\left(s_{z,t};\gamma_z,c_z\right) + \varepsilon_{z,t} \tag{7}$$

where, $G\left(s_{y,t};\gamma_y,c_y\right)$ is a scalar, meaning that the transition functions are common across equations.

Whether or not STAR-type nonlinearity is an adequate feature of the data-generating process, is a hypothesis to be tested. A conventional approach with the standard test statistics, however, cannot be employed, due to the so-called Davies's problem (e.g., Davies, 1977, 1987). For example, consider equation (7) in conjunction with equation (3): the nonlinear STAR(p) will reduce to the linear AR(p) either by imposing $\gamma = 0$ or by imposing $\alpha_1 = \beta_{1,1} = \ldots = \beta_{p,1} = 0$. Thus, γ is an unidentified nuisance parameter. Luukkonen et al. (1988) proposed a solution to the problem by approximating the transition function using Taylor series expansion. This, in turn, results in an auxiliary equation:

$$z_t = \varphi_0 + \sum_{j=0}^{3}\sum_{i=1}^{p} \varphi_{i,j} z_{t-i} s_t^j + \xi_t \tag{8}$$

where ξ_t combines the original error term, ε_t, and the approximation error resulted from the Taylor series expansion. Conventional testing methods can now be applied to equation (8). In particular, the linearity test is equivalent to testing the null hypothesis of: $\varphi_{i,1} = \varphi_{i,2} = \varphi_{i,3} = 0$, $i = 1, \ldots, p$. In small samples an F version of the LM statistics are used to test the null hypothesis of linearity. See Teräsvirta (1994) for additional details.

A similar approach can be applied to test linearity in a multivariate setting (e.g., Camacho, 2004). Consider the system of auxiliary equations:

$$\boldsymbol{y}_t = \boldsymbol{\phi}_0 + \sum_{j=0}^{3}\sum_{i=1}^{p} \Phi_{i,j} \boldsymbol{y}_{t-i} s_t^j + \sum_{j=0}^{3}\sum_{i=1}^{p} \boldsymbol{\phi}_{i,j} z_{t-i} s_t^j + \boldsymbol{\zeta}_t \tag{9}$$

The nonlinearity test is equivalent to testing system-wide the null hypothesis of $\Phi_{i,1} = \Phi_{i,2} = \Phi_{i,3} = \mathbf{0}$ and $\boldsymbol{\phi}_{i,1} = \boldsymbol{\phi}_{i,2} = \boldsymbol{\phi}_{i,3} = \mathbf{0}$, $i = 1, \ldots, p$. In small samples the so-called "curse of dimensionality" comes into effect and may distort the standard LM test (e.g., Teräsvirta and Yang, 2014). In such situations the equation-by-equation approach can be applied, using the univariate testing procedure as described above.

Finally, the testing procedure can be extended to assess the hypotheses of no remaining nonlinearity, no residual autocorrelation, and no structural change, as the diagnostic testing sequence for the estimated two-regime STAR or VSTAR models. See van Dijk et al. (2002) for further details.

3 Data

This study applies monthly data ranging from January of 1982 to December of 2013, obtained from the National Oceanic and Atmospheric Administration and the International Grains Council. It uses the *Niño3.4* anomaly index as a proxy for the ENSO anomalies. The *Niño3.4* series are collected from the National Oceanic and Atmospheric Administration's Climate Prediction Center.[1] The index is derived from daily sea-surface temperature values interpolated from weekly measures obtained from both satellites and actual locations around the Pacific. The sea-surface temperature anomaly in a given month, then, is the deviation in that particular month from the average historic *Niño3.4* measure relative to the 1981–2010 base period.

The wheat price series are from the Argentinian, Australian, Canadian, European, and the United States markets.[2] The nominal prices were adjusted to the 2010 levels using United States Producer Price Index for all commodities, obtained from the United States Bureau of Labor Statistics. Finally, the real price series were transformed to natural logarithms, to mitigate potential heteroskedasticity in the series, to facilitate the interpretation of the impulse–responses in percentage terms, and to avoid any inadequate negative realization of the prices in the out-of-sample simulation analysis.

The considered time series are plotted in Figure 1. Several features of the data are immediately apparent. Firstly, wheat prices tend to co-move, and the occasional divergences are promptly followed by the convergences of the series. Secondly, there seems to be a negative correlation between the ENSO cycles and the wheat price cycles.

For the purposes of testing and forecast extrapolation the time series ought to be stationary. The augmented Dickey–Fuller (ADF) tests were applied to the series of ENSO and wheat prices to test the null hypotheses of unit root. The test results are presented in Table 1. There is overwhelming evidence against unit roots in the series. The rest of the modelling exercise is, therefore, carried out using variables in levels.

[1] Available online at http://www.cpc.ncep.noaa.gov/data/indices/sstoi.indices.

[2] Several observations were missing from the raw data. The missing observations were interpolated by regressing the series of interest on the nearby futures prices of the soft red winter wheat as quoted on the Chicago Board of Trade, while controlling for the seasonal variation.

4 Model Selection, Estimation, and Interpretation

Following Brunner (2002), ENSO is assumed weakly exogenous to wheat prices. As such, $z_t = f(z_{t-1}, z_{t-2}, \ldots, \boldsymbol{d}_t)$ and $\boldsymbol{y}_t = g(\boldsymbol{y}_{t-1}, \boldsymbol{y}_{t-2}, \ldots, z_t, z_{t-1}, \ldots, \boldsymbol{d}_t)$ are considered, where z_t denotes the sea-surface temperature anomaly at time t, $\boldsymbol{y}_t = (p_t^{\text{USA}}, p_t^{\text{EUR}}, p_t^{\text{AUS}}, p_t^{\text{CAN}}, p_t^{\text{ARG}})'$ is a vector of wheat prices, and $\boldsymbol{d}_t$ is a vector of deterministic (e.g., seasonal) components. The $f(\cdot)$ and $g(\cdot)$ may be linear or nonlinear functions.

The model selection algorithm is as follows. First, the autoregressive lag length is determined, both for the vector of prices and the ENSO variable, based on the multivariate Bayesian Information Criterion (BIC), and subject to no residual autocorrelation. The selected (autoregressive) structure of linear models are carried over in testing and estimation of the nonlinear alternatives. Once the autoregressive order is set, the null hypotheses of linearity are tested using the auxiliary regressions. If, based on the linearity test results, the STAR-type process appears to be the likely feature of model dynamics, the (vector) smooth transition models are then estimated. Finally, the estimated models are assessed for no remaining nonlinearity, structural change, or residual autocorrelation.

The candidate transition variables are the lagged values of the ENSO variable, z_{t-d}, where $d = 1, \ldots, p$, in the case of the ENSO equation, and $d = 0, \ldots, p$, in the case of the price equations. Based on the linearity test results (see Table 2), the following nonlinear models are selected:

$$\begin{aligned}\boldsymbol{y}_t =& \tilde{\boldsymbol{\alpha}}_0 + \sum_{i=1}^{3} \tilde{B}_{i,0} \boldsymbol{y}_{t-i} + \sum_{i=1}^{3} \tilde{\boldsymbol{\beta}}_{i,0} z_{t-i} + \Pi_0 \boldsymbol{D}_t + \\ &+ \left(\tilde{\boldsymbol{\alpha}}_1 + \sum_{i=1}^{3} \tilde{B}_{i,1} \boldsymbol{y}_{t-i} + \sum_{i=1}^{3} \tilde{\boldsymbol{\beta}}_{i,1} z_{t-i} + \Pi_1 \boldsymbol{D}_t \right) G\left(s_{y,t}, \gamma_y, c_y\right) + \boldsymbol{\varepsilon}_{y,t} \end{aligned} \tag{10}$$

$$z_t = \alpha_0 + \sum_{i=1}^{3} \beta_{i,0} z_{t-i} + \pi_0' \boldsymbol{d}_t + \left(\alpha_1 + \sum_{i=1}^{3} \beta_{i,1} z_{t-i} + \pi_1' \boldsymbol{d}_t \right) G\left(s_{z,t}; \gamma_z, c_z\right) + \varepsilon_{z,t} \tag{11}$$

where $s_{y,t} = z_{t-2}$ and $s_{z,t} = z_{t-3}$ are the selected transition variables; $\boldsymbol{D}_t$ and $\boldsymbol{d}_t$ are matrices and vectors of seasonal dummy variables; and the rest of the variables and parameters are as defined

previously. The estimated transition functions are:

$$G\left(s_{y,t}, \hat{\gamma}_y, \hat{c}_y\right) = \left\{1 + \exp\left[-\underset{(—)}{100}/\sigma_{s_{y,t}}\left(z_{t-2} + \underset{(—)}{0.92}\right)\right]\right\}^{-1} \tag{12}$$

$$G\left(s_{z,t}; \hat{\gamma}_z, \hat{c}_z\right) = \left\{1 + \exp\left[-\underset{(0.98)}{2.62}/\sigma_{s_{z,t}}\left(z_{t-3} + \underset{(0.16)}{0.12}\right)\right]\right\}^{-1} \tag{13}$$

The values in parentheses are asymptotic standard errors of the parameter estimates. In the case of price equations, the gridsearch routine was implemented to approximate the nonlinear least squares estimation of the VSTAR model. The approach, in principle, is similar to the so-called SlowShift algorithm suggested by Enders and Holt (2011), who note that "with fine enough grid the in-sample mean square prediction error will be effectively minimized". These estimated functions are presented in Figures 2 and 3. In both instances the smooth transition between the regimes is apparent. In the case of ENSO, the inflection point of the transition function is centered around zero; as such, the autoregressive dynamics differ between El Niño and La Niña regimes. In the case of the system of price equations, the estimated function identifies the "extreme" La Niña regime with distinct price dynamics, as compared to the "other" regime that includes El Niño and neutral conditions.

There are a number of ways to examine the dynamics of the estimated models. This study adopts the generalized impulse–response (GIR) functions of Koop et al. (1996) for this purpose. The method is imperative when dealing with nonlinear models, which are not invariant to the information set prior the shocks, the sign and magnitude of the shocks, as well as, the idiosyncratic disturbances that occur throughout the forecast horizon. Thus, a GIR at a horizon h, for a given shock ν_t, and a history ω_{t-1}, is defined as:

$$\text{GIR}\left(h, \nu_t, \omega_{t-1}\right) = E\left(y_{t+h}|\nu_t, \omega_{t-1}\right) - E\left(y_{t+h}|\omega_{t-1}\right) \tag{14}$$

Thus, GIR is a function of ν_t and ω_{t-1}, which, in turn, are realizations of random variables V_t and Ω_{t-1}. Therefore, GIR can also be given as a realization of a random variable:

$$\text{GIR}\left(h, V_t, \Omega_{t-1}\right) = E\left(y_{t+h}|V_t, \Omega_{t-1}\right) - E\left(y_{t+h}|\Omega_{t-1}\right) \tag{15}$$

The current exercise follows the simulation algorithm similar to Skalin and Teräsvirta (2002). First the ENSO impulse–responses are obtained using 50 randomly sampled (without replacement) histories as initial conditions, 40 randomly sampled (without replacement) impulses from the pool of residuals of the estimated model, and 200 randomly sampled (with replacement) vectors of idiosyncratic shocks of length equal to 36. This way, a sufficiently large number of extrapolates are computed for each history-shock combination to approximate the impulse–response densities at each horizon. The ENSO extrapolates are then embedded in the system of price equations, to obtain the wheat price extrapolates, using the sampling procedure similar to the aforementioned. Both ENSO and wheat price GIRs are obtained by averaging the realized extrapolates across the bootstrap iterations for given initial shock and history. The distribution functions of these GIRs carry the information on the dynamic effects of ENSO on wheat prices. For illustration purposes density GIRs for horizons $h = \{1, 4, 12, 24\}$ are presented in Figure 4.

The graphs illustrate the distributions of the GIRs converge to "spikes" at zero with the horizon length, which is indicative of the time series being stationary and ergodic (Dijk et al., 2000). There also seem to be asymmetries associated with positive and negative shocks, manifested in skewed and multimodal distributions. The sign–specific asymmetries can be better illustrated by conditioning the GIRs on the direction of shock. For example, GIRs associated with positive shocks are given by:

$$\text{GIR}\left(h, \nu_t^+, \Omega_{t-1}\right) = E\left(y_{t+h}|\nu_t \in V_t^+, \Omega_{t-1}\right) - E\left(y_{t+h}|\Omega_{t-1}\right) \tag{16}$$

where V_t^+ denotes the subset of positive surprises. GIRs associated with negative shocks, i.e. $\text{GIR}\left(h, \nu_t^-, \Omega_{t-1}\right)$, are obtained in a similar fashion. To generate these impulse–responses, a sample of 40 positive and 40 negative shocks are selected, such that $\sigma_\varepsilon \leq |\nu_t| \leq 3\sigma_\varepsilon$. The rest of the sampling procedure is the same as before. The mean GIRs from this exercise are illustrated in Figure 5.

Several features of interest should be noted. First of all, the La Niña shocks result in increased wheat prices, while the opposite effect is observed after the El Niño shocks. The magnitude and economic significance of these effects is somewhat modest, which is possibly due to the offsetting

effects of ENSO in different parts of the world. For example, while droughts in North America and Canada are associated with the La Niña phase of the phenomenon, in Australia the similar weather effect coincides with the El Niño phase.

Another interesting feature of the observed dynamics is that the GIRs after a positive shock are not mirror images of the GIRs after a negative shock. The sign-specific asymmetries become apparent in the intermediate run. On average, prices tend to increase at a higher rate after the La Niña shocks, as compared to their decrease after the El Niño shocks. This confirms anecdotal evidence that the La Niñas are, on average, more damaging than the El Niños, in regards to world wheat production.

The observed sign-specific asymmetries motivate an additional step in the impulse–response analysis. A question of interest at this point is, are there history-specific asymmetries in the wheat price dynamics? Such conditional GIRs can be derived by slightly augmenting the equation (15). In particular, GIRs are now conditioned on a subset of histories, Ω_r, while everything else remains to be the same as before:

$$\text{GIR}\left(h, V_t, \omega_{t-1}^r\right) = E\left(y_{t+h}|V_t, \omega_{t-1} \in \Omega_r\right) - E\left(y_{t+h}|\omega_{t-1} \in \Omega_r\right) \tag{17}$$

For the purposes of current study, two distinct regimes were identified. The "La Niña regime", i.e. when $z_{t-3} < \hat{c}_z$ and $z_{t-2} < \hat{c}_y$, and the "El Niño regime". Twenty five histories are randomly sampled (without replacement) from each of these regimes. The rest of the bootstrap simulation algorithm is the same as before. As such, two more sets of GIRs are generated, and illustrated in Figures 6 and 7.

Additional interesting dynamic characteristics are revealed from these graphs. Firstly, the ENSO impulse–responses confirm a relatively abrupt mean-reversion during the El Niño regime, but a more persistent adjustment to the long-run mean with an indication to the so-called "double-dip" during the La Niña conditions. These, in turn, result in asymmetric effects on wheat price dynamics. A rather curious outcome is observed. During the La Niña phase, the magnitude of ENSO effect on wheat prices varies across countries. The effect is particularly apparent in the case of Canadian wheat, where prices deviate by approximately seven percent in the short run. For

the most part, however, the GIRs are largely statistically insignificant. On the contrary, during the El Niño phase, the GIRs are statistically significant, although the effects are economically less pronounced. Also, the responses to ENSO shocks follow a somewhat similar pattern across all considered regions.

Overall, La Niña episodes appear to increase wheat prices, and, in turn, prices tend to be more volatile during the La Niña regime. This finding is consistent with the economics of storage behavior (e.g., Wright, 2011, 2012). For example, if the global weather conditions associated with the La Niña episode cumulatively impact wheat production negatively, the international grain reserves will deteriorate. In such a situation, any further ENSO-driven shocks will have more amplified price responses.

5 Conclusion

Using over three decades of monthly data and the smooth transition modelling methodology, this study examines ENSO-induced asymmetric price transmissions in the international wheat market. The key findings of this research suggest that ENSO shocks affect wheat price dynamics, and more interestingly, there are indeed STAR-type regime-dependent nonlinearities in ENSO cycles as well as in the vector of wheat price series. This study finds that a positive ENSO shock, i.e. El Niño, results in decreased wheat prices, while a negative ENSO shock, i.e. La Niña, results in increased wheat prices. The average price responses to ENSO shocks vary across the considered export regions, but are all within three percent magnitude. Due to asymmetries, the La Niña effect is (in absolute terms) larger as compared to the El Niño effect, and, moreover, the responses are amplified during the La Niña regime, as compared to the El Niño regime. The latter finding is consistent with the economics of storage behavior, and is an indication of more fluctuating prices in the times of low grain stocks.

This analysis contributes to the growing literature in the economics of climate anomalies. It quantifies a rather nontrivial link between supply shocks due to ENSO anomalies, and the subsequent wheat price fluctuations. The analysis is carried out in a nonlinear setting. As such, this research uncovers some of the intricacies of ENSO–commodity price relationships, otherwise

camouflaged in a linear setting. The application and key findings of this study will interest researchers in the fields of climate economics and agricultural commodity price analysis. Moreover, because wheat is one of the most exported major staples around the world, this research also offers implications for international trade and development economics.

References

Balagtas, J. V. and M. T. Holt (2009). The Commodity Terms of Trade, Unit Roots, and Nonlinear Alternatives: A Smooth Transition Approach. *American Journal of Agricultural Economics 91*(1), 87–105.

Bessler, D. A., J. Yang, and M. Wongcharupan (2003). Price Dynamics in the International Wheat Market: Modeling with Error Correction and Directed Acyclic Graphs. *Journal of Regional Science 43*(1), 1–33.

Brunner, A. (2002). El Nino and World Primary Commodity Prices: Warm Water or Hot Air? *Review of Economics and Statistics 84*(1), 176–183.

Camacho, M. (2004). Vector Smooth Transition Regression Models for US GDP and the Composite Index of Leading Indicators. *Journal of Forecasting 23*(3), 173–196.

Cashin, P., C. J. McDermott, and A. Scott (2002). Booms and Slumps in World Commodity Prices. *Journal of Development Economics 69*(1), 277–296.

Chan, K. and H. Tong (1986). On Estimating Thresholds in Autoregressive Models. *Journal of time series analysis 7*(3), 179–190.

Critchlow, A. (2014). Food Price Alert as Experts Warn of New El Niño. *The Telegraph*. April 27, 2014.

Davies, R. (1977). Hypothesis Testing when a Nuisance Parameter is Present only under the Alternative. *Biometrika 64*(2), 247–254.

Davies, R. (1987). Hypothesis Testing when a Nuisance Parameter is Present only under the Alternative. *Biometrika 74*(1), 33–43.

Dijk, D. J. C., P. H. Franses, and H. P. Boswijk (2000). Asymmetric and Common Absorption of Shocks in Nonlinear Autoregressive Models. Technical report, Econometric Institute Research Papers.

Eitrheim, O. and T. Teräsvirta (1996). Testing the Adequacy of Smooth Transition Autoregressive Models. *Journal of Econometrics 74*(1), 59–75.

Enders, W. and M. T. Holt (2011). Breaks, Bubbles, Booms, and Busts: The Evolution of Primary Commodity Price Fundamentals. MPRA Paper No. 31461.

Friedman, T. L. (2010). Global Weirding is Here. *New York Times*, A23. February 17, 2010.

Goodwin, B. K., M. T. Holt, and J. P. Prestemon (2011). North American Oriented Strand Board Markets, Arbitrage Activity, and Market Price Dynamics: A Smooth Transition Approach. *American Journal of Agricultural Economics 93*(4), 993–1014.

Goodwin, B. K. and N. E. Piggott (2001). Spatial Market Integration in the Presence of Threshold Effects. *American Journal of Agricultural Economics 83*(2), 302–317.

Goodwin, B. K. and T. C. Schroeder (1991). Price Dynamics in International Wheat Markets. *Canadian Journal of Agricultural Economics 39*(2), 237–254.

Hall, A., J. Skalin, and T. Teräsvirta (2001). A Nonlinear Time Series Model of El Niño. *Environmental Modelling & Software 16*(2), 139–146.

Holt, M. T. and L. A. Craig (2006). Nonlinear Dynamics and Structural Change in the U.S. Hog-Corn Cycle: A Time-Varying STAR Approach. *American Journal of Agricultural Economics 88*(1), 215–233.

Hsiang, S., K. Meng, and M. Cane (2011). Civil Conflicts are Associated with the Global Climate. *Nature 476*(7361), 438–441.

Iizumi, T., J.-J. Luo, A. J. Challinor, G. Sakurai, M. Yokozawa, H. Sakuma, M. E. Brown, and T. Yamagata (2014). Impacts of El Niño Southern Oscillation on the Global Yields of Major Crops. *Nature Communications 5*.

Keppenne, C. (1995). An ENSO Signal in Soybean Futures Prices. *Journal of Climate 8*(6), 1685–1689.

Koop, G., M. Pesaran, and S. Potter (1996). Impulse Response Analysis in Nonlinear Multivariate Models. *Journal of Econometrics 74*(1), 119–147.

Laosuthi, T. and D. D. Selover (2007). Does El Niño Affect Business Cycles? *Eastern Economic Journal 33*(1), 21.

Legler, D., K. Bryant, and J. O'Brien (1999). Impact of ENSO-related Climate Anomalies on Crop Yields in the U.S. *Climatic Change 42*(2), 351–375.

Luukkonen, R., P. Saikkonen, and T. Teräsvirta (1988). Testing Linearity Against Smooth Transition Autoregressive Models. *Biometrika 75*(3), 491–499.

Mallya, G., L. Zhao, X. Song, D. Niyogi, and R. Govindaraju (2013). 2012 Midwest Drought in the United States. *Journal of Hydrologic Engineering 18*(7), 737–745.

Mason, S. J. and L. Goddard (2001). Probabilistic precipitation anomalies associated with ENSO. *Bulletin of the American Meteorological Society 82*(4), 619–638.

Mohanty, S., W. H. Meyers, and D. B. Smith (1999). A Reexamination of Price Dynamics in the International Wheat Market. *Canadian Journal of Agricultural Economics 47*(1), 21–29.

Mohanty, S., E. W. F. Peterson, and N. C. Kruse (1995). Price Asymmetry in the International Wheat Market. *Canadian Journal of Agricultural Economics 43*(3), 355–366.

Nicholls, N. (1985). Impact of the Southern Oscillation on Australian Crops. *Journal of Climatology 5*(5), 553–560.

Ropelewski, C. and M. Halpert (1987). Global and Regional Scale Precipitation Patterns Associated with the El Niño/Southern Oscillation. *Monthly Weather Review 115*(8), 1606–1626.

Rosenzweig, C., A. Iglesias, X. Yang, P. R. Epstein, and E. Chivian (2001). Climate Change and Extreme Weather Events: Implications for Food Production, Plant Diseases, and Pests. *Global Change & Human Health 2*(2), 90–104.

Rothman, P., D. van Dijk, and P. H. Franses (2001). Multivariate STAR Analysis of Money–Output Relationship. *Macroeconomic Dynamics 5*(4), 506–532.

Selvaraju, R. (2003). Impact of El Niño–Southern Oscillation on Indian Foodgrain Production. *International Journal of Climatology 23*(2), 187–206.

Skalin, J. and T. Teräsvirta (2002). Modeling Asymmetries and Moving Equilibria in Unemployment Rates. *Macroeconomic Dynamics 6*(2), 202–241.

Teräsvirta, T. (1994). Specification, Estimation, and Evaluation of Smooth Transition Autoregressive Models. *Journal of the American Statistical Association 89*(425), 208–218.

Teräsvirta, T. and H. Anderson (1992). Characterizing Nonlinearities in Business Cycles using Smooth Transition Autoregressive Models. *Journal of Applied Econometrics 7*(S1), S119–S136.

Teräsvirta, T. and Y. Yang (2014). Linearity and Misspecification Tests for Vector Smooth Transition Regression Models. *CREATES Research Paper 4*.

Timmermann, A., J. Oberhuber, A. Bacher, M. Esch, M. Latif, and E. Roeckner (1999). Increased El Niño Frequency in a Climate Model Forced by Future Greenhouse Warming. *Nature 398*(6729), 694–697.

Tong, H. and K. S. Lim (1980). Threshold Autoregression, Limit Cycles and Cyclical Data. *Journal of the Royal Statistical Society. Series B (Methodological) 42*(3), 245–292.

Ubilava, D. and C. Helmers (2013). Forecasting ENSO with a Smooth Transition Autoregressive Model. *Environmental Modelling & Software 40*(1), 181–190.

Ubilava, D. and M. Holt (2013). El Niño Southern Oscillation and Its Effects on World Vegetable Oil Prices: Assessing Asymmetries using Smooth Transition Models. *Australian Journal of Agricultural and Resource Economics 57*(2), 273–297.

van Dijk, D., T. Teräsvirta, and P. Franses (2002). Smooth Transition Autoregressive Models–A Survey of Recent Developments. *Econometric Reviews 21*(1), 1–47.

Weise, C. (1999). The Asymmetric Effects of Monetary Policy: A Nonlinear Vector Autoregression Approach. *Journal of Money Credit and Banking 31*(1), 85–108.

Wright, B. D. (2011). The economics of grain price volatility. *Applied Economic Perspectives and Policy 33*(1), 32–58.

Wright, B. D. (2012). International grain reserves and other instruments to address volatility in grain markets. *The World Bank Research Observer 27*(2), 222–260.

Figures

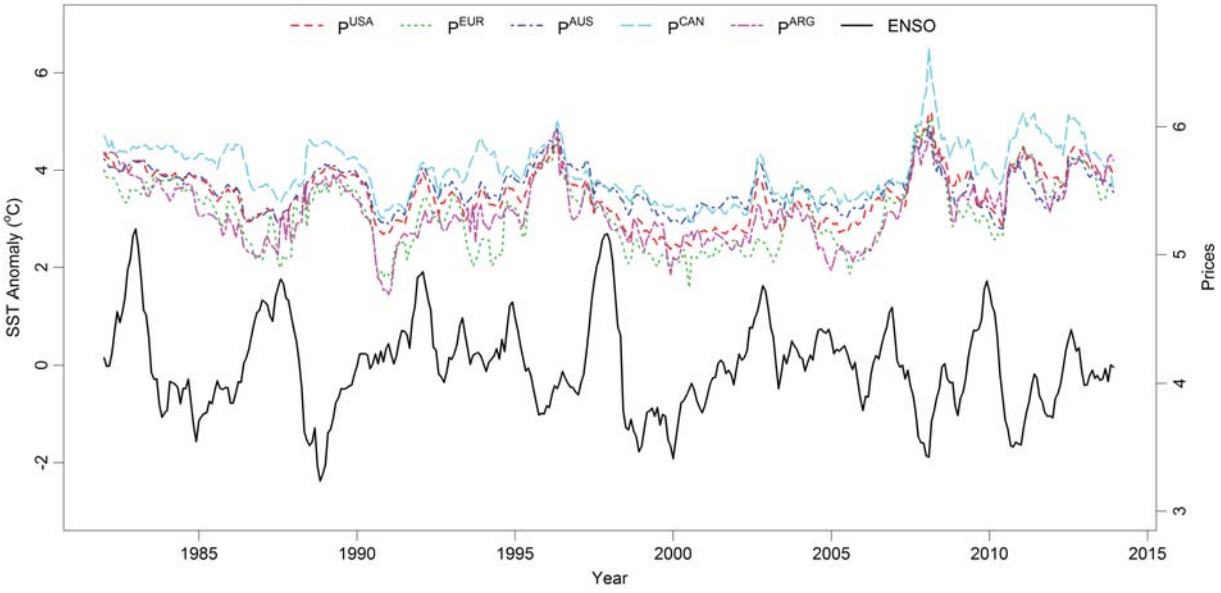

Note: The prices are natural logarithms of the real wheat prices.

Figure 1: Monthly Series of ENSO and Wheat Prices

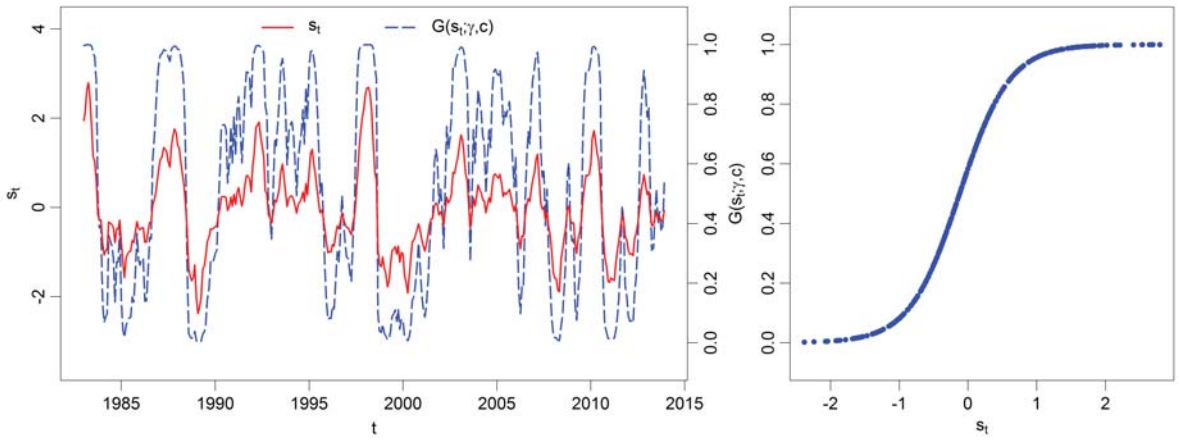

Figure 2: The Estimated Transition Function for ENSO Equation

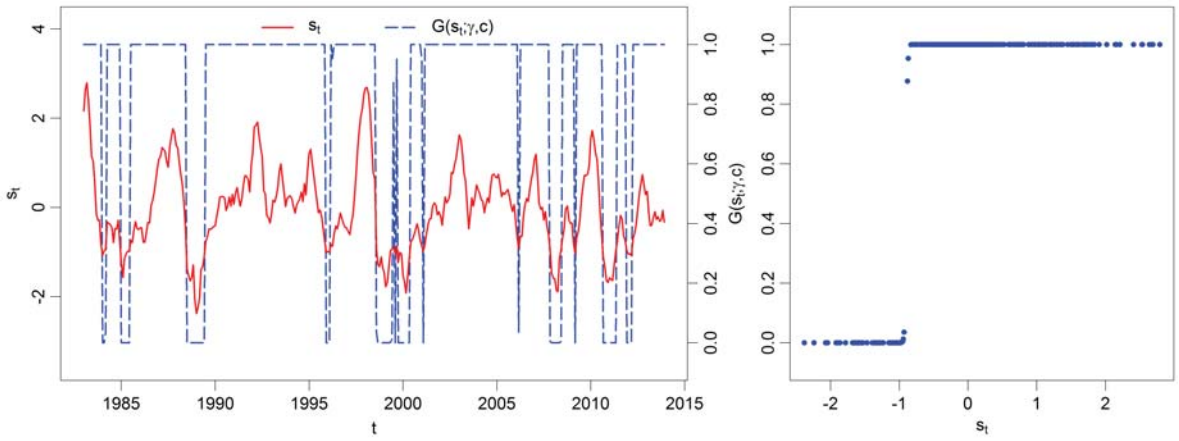

Figure 3: The Estimated Transition Function for System of Price Equations

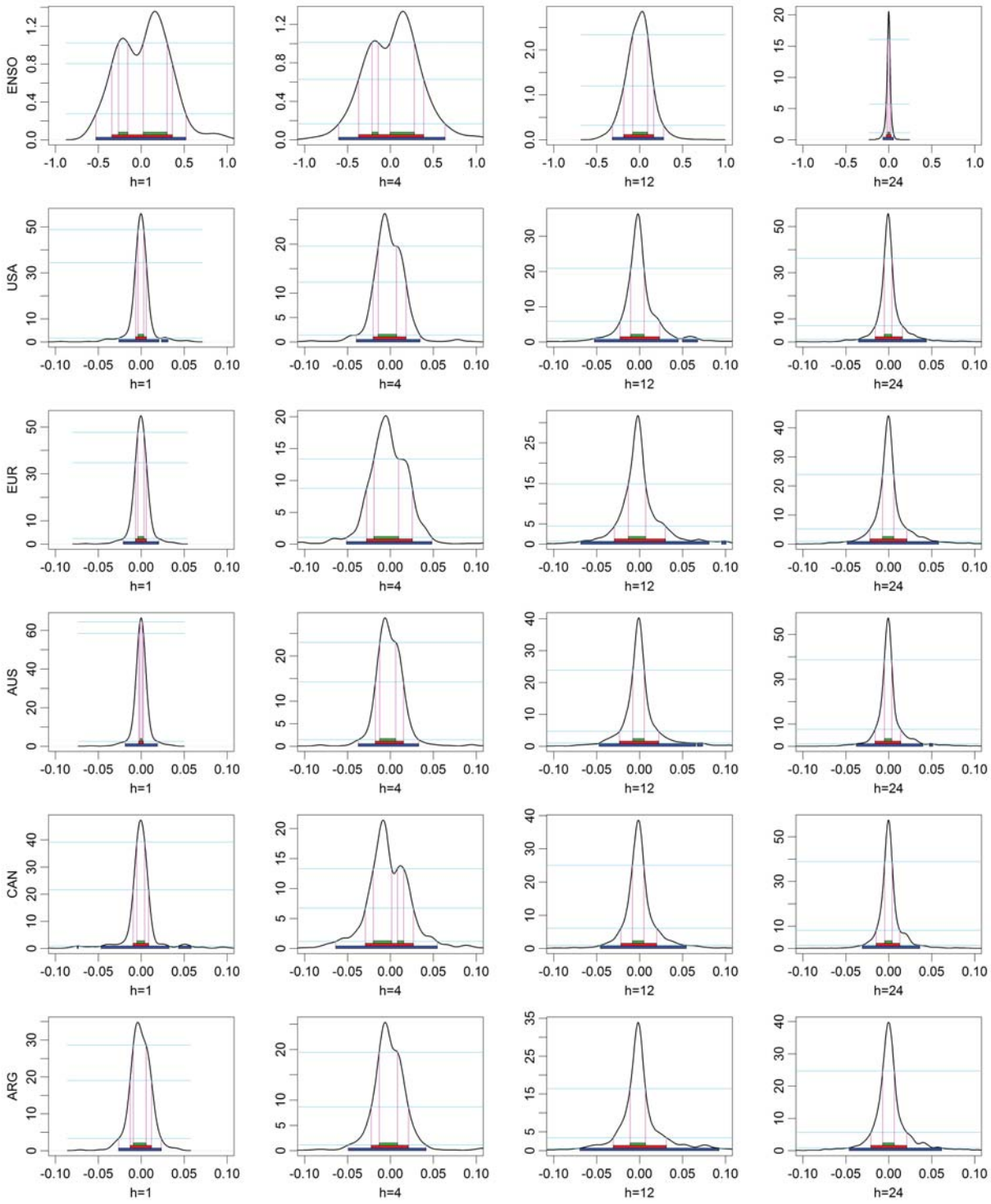

Figure 4: Density Generalized Impulse–Responses

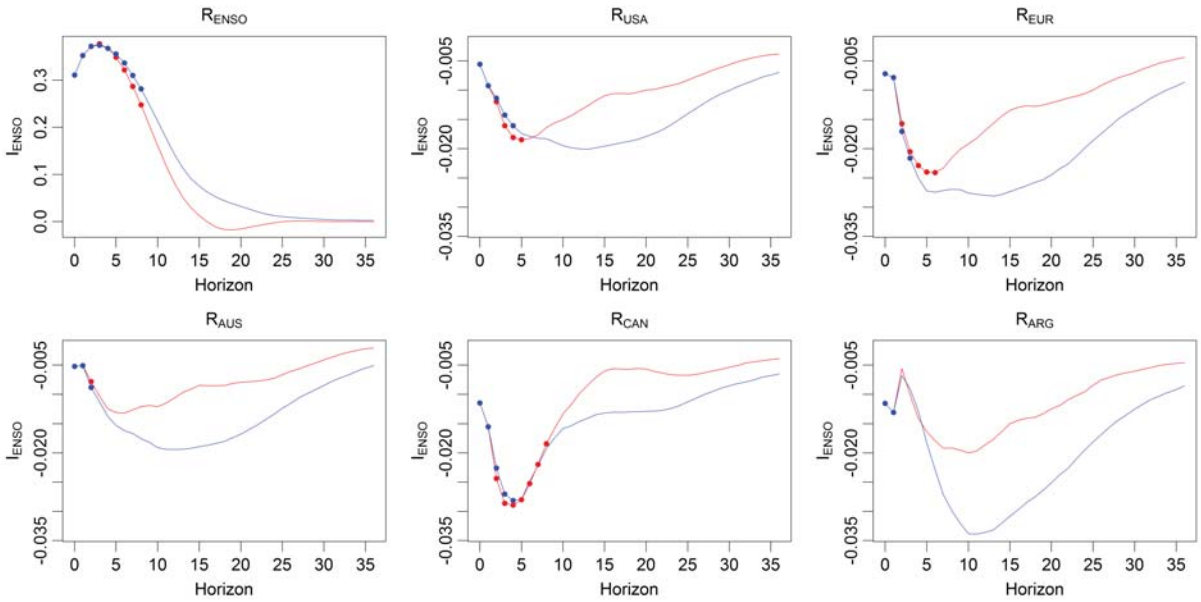

Note: GIRs in red are associated with the El Niño shocks, and GIRs in blue are associated with the La Niña shocks. GIRs associated with the La Niña shocks are multiplied by negative one, and thus inverted, to facilitate the comparison with the analogous (but opposite in sign) El Niño shocks. Dots denote instances when zero doesn't fall within the 90 percent confidence interval.

Figure 5: Mean Generalized Impulse–Responses

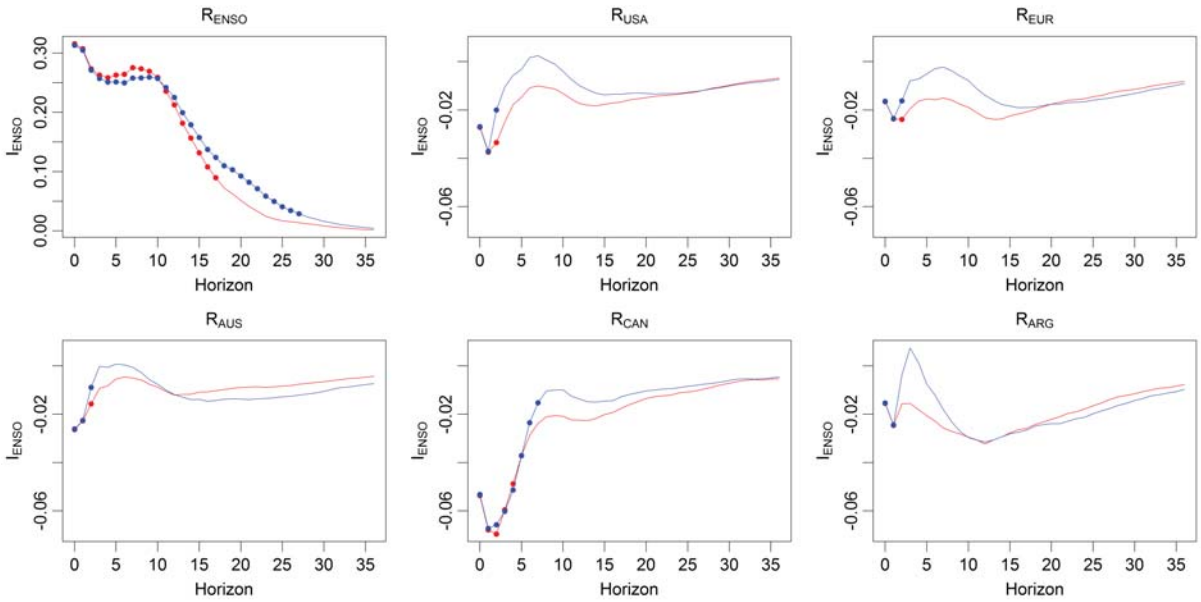

Note: See Figure 5

Figure 6: Generalized Impulse–Responses during the La Niña Regime

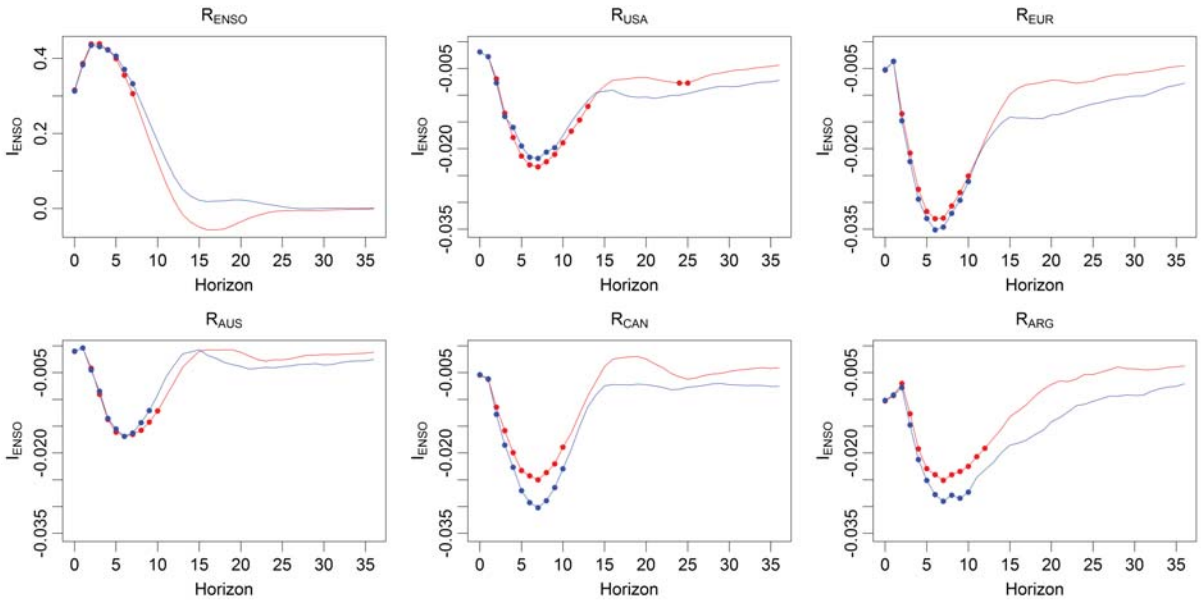

Note: See Figure 5

Figure 7: Generalized Impulse–Responses during the El Niño Regime

Tables

Table 1: Unit Root Test Results for ENSO and Wheat Price Series

Statistic	ENSO	USA	EUR	AUS	CAN	ARG
ADF_L	**-5.58**	*-3.42*	**-3.51**	**-4.23**	**-3.72**	*-3.13*
ADF_Δ	**-8.55**	**-10.78**	**-10.40**	**-10.44**	**-10.46**	**-10.77**

Note: Table entries are statistics associated with the null hypotheses of unit root in the augmented Dickey–Fuller (ADF) tests. Subscripts L and Δ denote whether the series being tested are in levels or in first-differences. Italics denote statistical significance at $\alpha = 0.05$ level, and bolds denote statistical significance at $\alpha = 0.01$ level.

Table 2: Diagnostic Test Results for Estimated Smooth Transition Models

Statistic	ENSO	USA	EUR	AUS	CAN	ARG
			No Remaining Nonlinearity			
z_t		0.129	0.099	0.052	0.046	0.024
z_{t-1}	0.170	0.375	0.045	0.162	0.089	0.073
z_{t-2}	0.450	0.717	0.458	0.298	0.188	0.241
z_{t-3}	0.099	0.974	0.942	0.897	0.347	0.268
			No Structural Change			
t^*	0.260	0.165	0.004	0.018	0.143	0.372
			No Serial Correlation			
ac_{t-1}	0.023	0.168	0.760	0.768	0.525	0.560
ac_{t-6}	0.282	0.372	0.902	0.267	0.154	0.255
ac_{t-12}	0.322	0.053	0.468	0.174	0.006	0.609
			No Conditional Heteroskedasticity			
$arch_{t-1}$	0.252	0.014	0.066	<0.001	0.160	<0.001
$arch_{t-6}$	0.858	0.003	0.035	0.004	0.534	0.001
$arch_{t-12}$	0.647	<0.001	0.002	0.003	0.800	<0.001

Note: Table entries are asymptotic probability values of the associated null hypotheses.